11/5/09

Resonant magnetic perturbation experiments on MAST using external and internal coils for ELM control

A. Kirk, E. Nardon, R. Akers, M. Bécoulet[a], G. De Temmerman, B. Dudson[b], B. Hnat[c], Y.Q. Liu, R. Martin, P. Tamain, D. Taylor and the MAST team

EURATOM/UKAEA Fusion Association, Culham Science Centre, Abingdon, Oxon OX14 3DB, UK

[a]*Association Euratom/CEA, CEA Cadarache, F-13108, St. Paul-lez-Durance, France*

[b]*University of York, Heslington, York YO10 5DD UK*

[c]*Centre for Fusion, Space and Astrophysics, Warwick University, Coventry CV4 7AL, UK*

Abstract

Experiments have been performed on MAST using both external (n=1,2) and internal (n=3) resonant magnetic perturbation coils. ELM suppression has not been achieved even though vacuum modelling shows that either set of coils can produce a region for which the Chirikov parameter is greater than 1 wider than that required to produce ELM suppression in DIII-D. Hence having a certain width of the edge stochastic region may be a necessary criterion but is not a sufficient condition to ensure ELM suppression on any device. Although complete ELM suppression has not been achieved some effects on the ELMs have been observed including triggering ELMs in ELM free H-mode periods and increasing the ELM frequency in regularly ELMing discharges. In addition, large changes to the edge turbulence have been observed in L-mode discharges.

1. Introduction

All current estimations of the energy released by type I ELMs indicate that in order to ensure an adequate lifetime of the divertor targets on ITER a mechanism to decrease the amount of energy released by an ELM, or to eliminate ELMs altogether is required [1]. One such amelioration mechanism relies on perturbing the magnetic field in the edge plasma region, enhancing the transport of particles or energy and keeping the edge pressure gradient below the critical value that would trigger an ELM while still maintaining an edge transport barrier. This technique of Resonant Magnetic Perturbations (RMPs) has been successfully employed on DIII-D using two up-down symmetric sets of 6 in-vessel coils [2] and more recently on JET using the external error field correction coils [3]. On DIII-D, complete ELM suppression has been possible, whereas on JET only ELM mitigation (increased frequency and decreased energy loss) has been obtained. MAST is equipped with both a set of ex-vessel error field correction coils (EFCCs), similar to JET, and more recently with a set of 12 in-vessel coils, similar to those used in DIII-D.

The MAST error field correction system consists of four coils arranged symmetrically around the outside of the vacuum vessel at a radius of 2.9 m. Each coil is ~ 4m high, consists of three turns and can carry up to 5 kA/turn. Opposite coils are normally wired in pairs to produce a non-axisymmetric magnetic field with a dominant n=1 component [4]. The internal coils are constructed from an aluminium alloy and are composed of 4 turns each and are designed to carry currents up to 2 kA/turn, although the current power supplies are limited to 1.4 kA. The coils measure 270 by 600 mm and are arranged in two equally spaced toroidal rows of 6 one above and one below the midplane (for their poloidal location see Figure 1). To electrically insulate the coils, they are coated in aluminium oxide and are then encased inside a boron nitride shell, which is then coated in colloidal graphite. The coils can be

operated in either "even" parity (where the currents in the upper and lower coil at the same toroidal location have the same sign) or "odd" parity (the currents in the upper and lower coil have opposite sign).

Plasmas in MAST typically have a major radius, $R \sim 0.8$ m and a minor radius, $a \sim 0.55$ m. The internal and external coils have been applied to a range of L-mode and ELMy H-mode discharges when the plasma is either near to a Connected Double Null (CDN) or in a Lower Single Null Divertor (SND) configuration with the ion ∇B drift direction towards the lower targets (i.e. towards the "active" X-point). The discharges have a range of parameters with plasma current (I_P)~0.4-0.9 MA, Greenwald density ~0.2-0.9, elongation ~1.6-2.1, triangularity ~0.3-0.52 and q_{95} ~3-7 and neutral beam heating powers (P_{NBI}) up to 3.8 MW. The toroidal field on axis is in the range $0.45\ T < B_\phi < 0.55\ T$. In this paper the results from four scenarios will be presented. The poloidal cross section, together with the location of the internal coils, for these scenarios is shown in Figure 1 (the external coils, which are not shown, are located at a radius of 2.9 m). Scenario 1 is a CDN Ohmic discharge with I_P = 400 kA, B_T = 0.52 T and q_{95}= 6, scenario 2 is a neutral beam heated CDN discharge with I_P = 680 kA, B_T = 0.55 T and q_{95}= 5.5, scenario 3 is a larger radius neutral beam heated CDN discharge with I_P = 750 kA, B_T = 0.55 T and q_{95}= 5 and scenario 4 is a neutral beam heated SND discharge with I_P = 600 kA, B_T = 0.52 T and q_{95}= 3.

2. *H-mode experiments using the external Error Field Correction Coils (EFCC) (n=1,2)*

Initial ELM mitigation experiments were performed using a n=1 field from the ex-vessel coils. The current in one or both pairs of coils was increased/decreased from its original error field correction value. In all cases this configuration of the coils produced a delay in the L-H transition if the coils were applied too early in the discharge, with the length

of the delay increasing with the size of the applied current. This is demonstrated in Figure 2 in which coil currents of 1.0, 2.0, 2.5 and 4.0 kA are applied to a "scenario 2" discharge with P_{NBI} = 2 MW. The maximum coil current of 4 kA delays the time of the L-H transition, at constant input power, by ~60 ms. The location of the coils outside the vacuum vessel and the penetration time of the field through the metal walls, means that the field at the plasma reaches its maximum ~ 50 ms after the peak in the coil current. In subsequent experiments the coils were energised taking into account this delay, such that the peak field was not reached until after the L-H transition.

In n=1 experiments, however, it was difficult to find an operational window where sufficient current could be applied without either causing a back transition H-L or a low m locked mode (from the magnetic signals it appears to be an m=2, n=1 mode at q=2) . This is somewhat similar to the behaviour seen on JET, where at low q_{95} a narrow window in EFCC current was found between ELM mitigation and locked mode onset.

Experiments were also performed using an n=2 configuration, where 2 of the four error field coils were re-wired in parallel to produce a dominantly n=2 harmonic perturbation and the remaining 2 coils were left wired in an anti-parallel configuration to cancel the n=1 component of the intrinsic error field. Calculations of the perturbation to the plasma for 15 kA turns (kA.t) in the coils have been performed using the ERGOS code (vacuum magnetic modelling) [5]. The stochastic layer is defined as the region for which the Chirikov parameter (σ_{ch}) is greater than 1 [5]. The σ_{Ch} profile for the case with I_{EFCC}=15kAt applied to a "scenario 3" discharge is presented in Figure 3 together with profiles from shots on DIII-D and JET in which ELM mitigation has been observed [6]. The MAST profile is clearly above the DIII-D and JET profiles. This is due to the large magnetic shear at the edge of MAST, which makes island overlap easier. The Chirikov parameter is greater than 1 when $\psi_{pol}^{1/2} > 0.91$ (where Ψ_{pol} is the normalised poloidal flux) i.e. the region of flux space from the

edge of the plasma that is thought to be stochastic satisfies $\Delta\Psi_{pol} > 0.17$. On DIII-D it has been found that complete suppression of type I ELMs can be established using their internal coils when $\Delta\Psi_{pol} > 0.165$ [7]. Hence if the width of edge stochastic region in normalised flux was the only criterion that needed to be satisfied, a suppression of Type I ELMs would be expected on MAST.

Figure 4 shows the results obtained by applying an n=2 perturbation in a series of low pedestal collisionality ($\nu_e^*=0.3$) "scenario 3" discharges with P_{NBI} =3.2 MW using EFCCs currents of I_{EFCC}=0 (for reference), 12, and 15kAt. Notice that the ELMs in this type of discharge have a high natural frequency (~500Hz) and cannot be classified as Type I ELMs. Nevertheless, the EFCCs were observed to increase their frequency by typically 50 %. The evolution of the line integrated density shows that the EFCCs produce a drop in density, which is reminiscent of the density pump-out observed in experiments on DIII-D [2] and JET [3]. The density pedestal decreases by ~ 20 % in this period whilst the electron temperature pedestal remains unchanged. No effect is observed on the divertor strike points, in particular there is no evidence for the strike point splitting which has been observed on DIII-D during the application of RMPs [8].

The fact that ELM suppression is not observed here could be due to the fact that these ELMs are not Type I ELMs, but also to the limited relevance of the vacuum modelling, or to the fact that the width of the edge stochastic region by itself is not sufficient for ELM suppression. It is interesting to note that, to date, complete suppression has not been observed on any device using a single row of mid-plane coils.

3. L-mode experiments using the internal coils (n=3)

Following the installation of the internal coils, experiments were initially performed in Ohmic "Scenario 1" discharges. Calculations of the perturbation to the plasma from these coils have again been performed using the ERGOS code. Figure 5a and b show the poloidal magnetic spectra of the applied perturbation (b^1) as a function of poloidal mode number (m) and normalised radius ($\Psi_{pol}^{1/2}$) for even and odd parity coil configurations respectively. b^1 represents the normalised perpendicular component of the perturbed field and is given by $b^1 \equiv \left(\vec{B}\cdot\vec{\nabla}\psi_{pol}^{1/2}\right)\Big/\left(\vec{B}\cdot\vec{\nabla}\varphi\right)$ where $\vec{B}$ is the total field vector and φ is the toroidal angle [9]. Superimposed on the spectra are the location of the q=m/3 rational surfaces. The q_{95} in these plasmas is higher (6-8) than that in normal H-mode plasmas and as such the applied perturbation is resonant in the even configuration i.e. the rational surface locations are well aligned with the peaks in the applied perturbation. Figure 5c shows the predicted Chirikov parameter profile for the even and odd parity configurations. For the same current in the coils the Chirikov parameter is much larger in the even parity configuration and can produce $\sigma_{Ch}>1$ for $\psi_{pol}^{1/2} > 0.9$.

Figure 6 shows the effect of applying 1.4 kA (5.6 kA turns (kA.t)) in the coils in the two configurations to the Ohmic "Scenario 1" discharge. The odd parity configuration has no effect on the plasma while in the even parity configuration a clear and repeatable reduction in the density was observed. Although the density is reduced there is little effect on the electron temperature which is measured using a Thomson scattering system. The effect of the coils on the edge turbulence was investigated by studying the ion saturation current measured by a Langmuir probe located on the head of a reciprocating probe. The probe was reciprocated ~1

cm inside the Last Closed Flux Surface (LCFS). In order to isolate the changes due to density, the discharge without the coils was repeated at the density achieved following the application of the coils. The mean of the I_{SAT} traces were similar and in the Scrape Off Layer (SOL) the Probability Distribution Functions (PDFs) were also similar. However, inside the LCFS the distributions were very different. Although the mean was the same there was a large difference in the width (RMS) and asymmetry (Skewness). In the case where the coils were applied the RMS increased by a factor of 2 while the skewness and kurtosis decreased. This may imply that a different type of turbulence is dominant in the presence of the stochastic fields. In addition, the rotation of the edge plasma has been determined by tracking the toroidal propagation of the filaments observed in visible imaging using the technique used on previous L-mode [10] and inter-ELM discharges [11]. Firstly the L-mode filaments are still observed in the presence of the applied field, however, the toroidal rotation of the filaments is observed to decrease from 7 to 4 kms^{-1} as the coils are energised. There is also some evidence for modification of the divertor target profiles (so called strike point splitting), in that during energisation of the coils lobes are observed in the divertor heat flux profiles measured using Infrared thermography.

4. H-mode experiments using the internal coils (n=3)

The initial H-mode experiments were performed in "Scenario 2" CDN discharges with 1.8 MW of neutral beam heating. In this discharge the $q_{95} \sim 5.5$ during the H-mode period. The ERGOS modelling shows that the Chirikov parameter is slightly higher for odd parity compared to even parity (Figure 7c). However, as can be seen from Figure 7a and b the plasma resonances (shown by the crosses) are not perfectly aligned with the ridge in the applied magnetic perturbation spectrum for either parity. Similar to what has been observed on NSTX using external coils in an n=3 configuration [12], it is possible to trigger high

frequency ELMs in a discharge that was initially in an ELM free H-mode state. In the initial experiments, which used an effective square wave current trace in the coils (i.e. the coil current was ramped to its pre-set maximum and then held constant) ELMs were triggered but this was quickly followed by a back transition to L-mode. The length of the ELM-ing period could be maximised if the current waveform was changed to one in which the current was quickly ramped up to its pre-set maximum value and then slowly reduced. An example of such a waveform and its effect on a discharge that without current in the coils was ELM free is shown in Figure 8. The need for a reduction in the coil current after an initial maximum suggests that a field penetration effect is involved i.e. a certain field strength is required to enable the field to penetrate the plasma edge, however, once this field has penetrated the islands produced are too large and effect the H-mode barrier resulting in a back transition to L-mode. If the field is reduced the resulting island size is reduced and the H-mode can be sustained.

If the coils are applied to a discharge with frequent type III ELMs, firstly a set of compound ELMs are produced but at higher coil currents the plasma reverts to a dithering state, similar to what is observed if the heating power is only just above that required for the L-H transition. Experiments have also been performed in discharges with regular type I ELMs. Figure 9a and b show the poloidal magnetic spectra for the coils in even and odd parity respectively for a "Scenario 3" discharge. Although the perturbation spectrum is not well aligned with the plasma resonances, when the current in the coils is 1.4 kA (5.6 kA.t), the Chirikov parameter (Figure 9c) is greater than 1 for both odd and even parity when $\psi_{pol}^{1/2} > 0.91$, i.e. the region of flux space from the edge of the plasma that is stochastic satisfies $\Delta\Psi_{pol} > 0.17$, which is larger than the region required on DIII-D to produce complete ELM suppression [7].

Figure 10 shows the effect of applying the coils in even or odd parity to this scenario, which uses 3.4 MW of neutral beam heating. The q_{95} of this discharge is 5.0 and the pedestal collisionality (ν^*_{ped}) is 0.5. No effect is observed on the density or the ELM behaviour in either parity. This shows that although the criterion of $\Delta\Psi_{pol}$ >0.165 may be necessary to suppress ELMs on DIII-D it is not sufficient to produce ELM mitigation on all devices. In addition, the application of the coils does not cause any braking to the toroidal rotation of the plasma, i.e. there is no evidence of Neoclassical Toroidal Viscosity (NTV) braking [13].

This is not always the case as considerable plasma braking has been observed in a "Scenario 4" plasma. In this lower SND magnetic configuration the plasma is far from the upper row of coils (see Figure 1) and hence the perturbation is effectively only from the lower row of coils. This produces a much broader spectrum of magnetic perturbation as shown in Figure 11a. However, for the maximum coil current of 1.4 kA (5.6 kA.t) a large region for which σ_{Ch}>1 can still be produced (Figure 11b). The coils have been applied to such a discharge with 3.2 MW of neutral beam heating. This type I ELMing discharge has q_{95} ~ 3.0 and ν^*_{ped} ~ 0.5. Figure 12a shows the effect of applying a coil current of 1 kA (4 kA.t) in the lower row of coils: an increase in the ELM frequency and decrease of the ELM size is observed, together with a decrease in the plasma density. Unfortunately this is then followed by a back transition to L-mode at ~ 0.41 s. Figure 12b and c show the radial profiles of toroidal velocity measured using charge exchange recombination spectroscopy for the time periods indicated in Figure 12a for the discharge without and with the coils respectively. For the discharge without the coils (Figure 12b) there is very little change in the toroidal velocity profiles, however, for the discharge with the coils energised (Figure 12c) a rapid drop in the toroidal velocity is observed extending all the way into the core of the plasma. The velocity starts to decrease as soon as the coils are turned on and continues to decrease, reaching approximately zero at a radius of 1.15 m at the time of the back transition to L-mode, which

occurs at ~ 0.41 s. This is similar to what has been observed in NTV braking experiments on NSTX [13]. NTV braking may have a larger effect in these discharges due to the broader poloidal spectrum of the magnetic perturbation. To date it has not been possible to produce a suitable waveform for the coil current that can reduce the ELM size but avoid a back transition to L-mode.

5. Summary and conclusions

Experiments have been performed on MAST using both external (n=1 or 2) and internal (n=3) resonant magnetic perturbation coils. Vacuum modelling with ERGOS shows that either set of coils can produce a region for which the Chirikov parameter is greater than 1 which is wider than that required to produce ELM suppression in DIII-D and ELM mitigation in JET. Hence if the width of the vacuum field predicted edge stochastic region is the only condition that is required to suppress ELMs then it is should be reproducible on MAST. When the external coils were in a n=1 configuration it was not possible to find an operational window in which the required current could be applied without producing a back transition from H to L-mode. In an n=2 configuration of the external coils it was possible to increase the ELM frequency from 500 to 700 Hz but ELM suppression was not established. The internal coils can produce a reduction in the density in Ohmic L-mode plasmas provided there is a good alignment between the plasma rational surfaces and the applied perturbation. Applying the n=3 internal coils to a 750 kA CDN H-mode plasma it is possible to obtain a Chirikov parameter greater than 1 for a region of flux space $\Delta\Psi_{pol} > 0.17$ without having any effect on the ELMs. Hence it has been possible to establish that the width of the vacuum field predicted stochastic layer required on DIII-D for ELM suppression [7], maybe necessary, but is not a sufficient criterion to ensure ELM suppression on all devices. However, it should be

noted that there is not yet any evidence that the vacuum field predictions translate to a stochastic layer in the experiment. In an SND plasma it has been possible to decrease the ELM size and produce a density pump-out. However, the plasma rotation is also strongly reduced and a back transition to L-mode occurs.

Acknowledgements

UKAEA authors were funded jointly by the United Kingdom Engineering and Physical Sciences Research Council and by the European Communities under the contract of Association between EURATOM and UKAEA. The views and opinions expressed herein do not necessarily reflect those of the European Commission.

References

[1] Loarte A *et al.*, 2003 Plasma Phys. Control. Fusion **45** 1594

[2] Evans T. *et al.*, 2004 Phys. Rev. Lett. **92** 235003

[3] Liang Y. *et al.*, 2007 Phys. Rev. Lett. **98** 265004

[4] Howell D.F. et al., 2007 Nucl. Fusion **47** 1336

[5] Nardon E. *et al*., 2007 *J. Nucl. Mater.* **363-365** 1071

[6] Nardon E. *et al*., 2008 "ELM control by resonant magnetic perturbations on JET and MAST", In press *J. Nucl. Mater.*

[7] Fenstermacher M.E. et al. 2008 Phys. of Plasma **15** 056122

[8] Schmitz O. *et al.*, 2008 Plasma Phys. Control. Fusion **50** 124029

[9] Nardon E. 2007 Edge Localized modes control by resonant magnetic perturbations *PhD Thesis* Ecole Polytechnique http://www.imprimerie.polytechnique.fr/Theses/Files/Nardon.pdf

[10] Dudson B. *et al.*, 2008 Plasma Phys. Control. Fusion **50** 124012

[11] Ben Ayed N. *et al.*, 2009 Plasma Phys. Control. Fusion **51** 035016

[12] Canik J et al., 2008 "Magnetic ELM Pace-making with 3-D Applied Fields in NSTX" PD/P1-5 presented at the 22nd IAEA Fusion energy conference, Geneva, Switzerland, 2008.

[13] W. Zhu *et al.*, 2006 Phys. Rev. Lett. **96** 225002

Figures

Figure 1 Poloidal profiles of the discharge scenarios. The location of the internal coils is also indicated. The external coils have a height of 4m and are located at a radius of 2.9 m.

Figure 2 Effect of increasing n=1 error field correction current on the time of the L-H transition for a "scenario 2" discharge.

Figure 3 Calculated Chirikov parameter profiles for a MAST "scenario 2" discharge using the external coils in a n=2 configuration. Superimposed are the profiles for DIII-D and JET discharges in which ELM mitigation has been established.

Figure 4 Effect of increasing n=2 error field correction current on a "scenario 3" H-mode plasma: The target D_α, ELM frequency (f_{ELM}) and line averaged density ($\bar{n}_e$) as a function of time.

Figure 5 Poloidal magnetic spectra for the a) even and b) odd parity configurations for a "scenario 1" discharge. Superimposed as crosses are the q=m/3 rational surfaces of the discharge equilibrium.c) Predicted profiles of the Chirikov parameter produced with 5.6 kA.t in the internal ELM coils in even (open circles) and odd (crosses) parity configurations.

Figure 6 Ohmic shot (scenario 1) with 400 kA plasma current using the internal coils in Odd and Even parity mode. a) the applied coil current (solid - LH axis) and q_{95} (dashed - RH axis). The line average density in b) Odd and c) Even parity mode shots with 0 (solid) and 1.4 kA (dashed) current in the coils.

Figure 7 Poloidal magnetic spectra for the a) even and b) odd parity configurations for a "scenario 2" discharge. Superimposed as crosses are the q=m/3 rational surfaces of the discharge equilibrium.c) Predicted profiles of the Chirikov parameter produced with 5.6 kA.t in the internal ELM coils in even (open triangles) and odd (solid triangles) parity configurations.

Figure 8 Comparison of "scenario 2" discharges with and without application of the internal coils in odd parity: line averaged density ($\bar{n}_e$), coil current (I_{ELM}) and target D_α as a function of time.

Figure 9 Poloidal magnetic spectra for the a) even and b) odd parity configurations for a "scenario 3" discharge. Superimposed as crosses are the q=m/3 rational surfaces of the discharge equilibrium.c) Predicted profiles of the Chirikov parameter produced with 5.6 kA.t in the internal ELM coils in even (open circles) and odd (crosses) parity configurations.

Figure 10 Time traces of line average density ($\bar{n}_e$), coil current (I_{ELM}) and D_α for a 3.2 MW Beam heated H-mode shot (Scenario 3) using the internal coils in even or odd parity mode.

Figure 11 a) Poloidal magnetic spectra for the lower row of coils a "scenario 4" discharge. Superimposed as crosses are the q=m/3 rational surfaces of the discharge equilibrium.

b) Predicted profile of the Chirikov parameter produced with 5.6 kA.t in the internal ELM coils.

Figure 12 a) Time traces of coil current (I_{ELM}), target D_α and line average density ($\bar{n}_e$) for a 3.2 MW beam heated H-mode shot (Scenario 4) using the lower row of the internal coils. b) and c) radial profiles of the toroidal velocity (V_ϕ) for the time period shown in a) for discharges with and without current in the coils respectively.

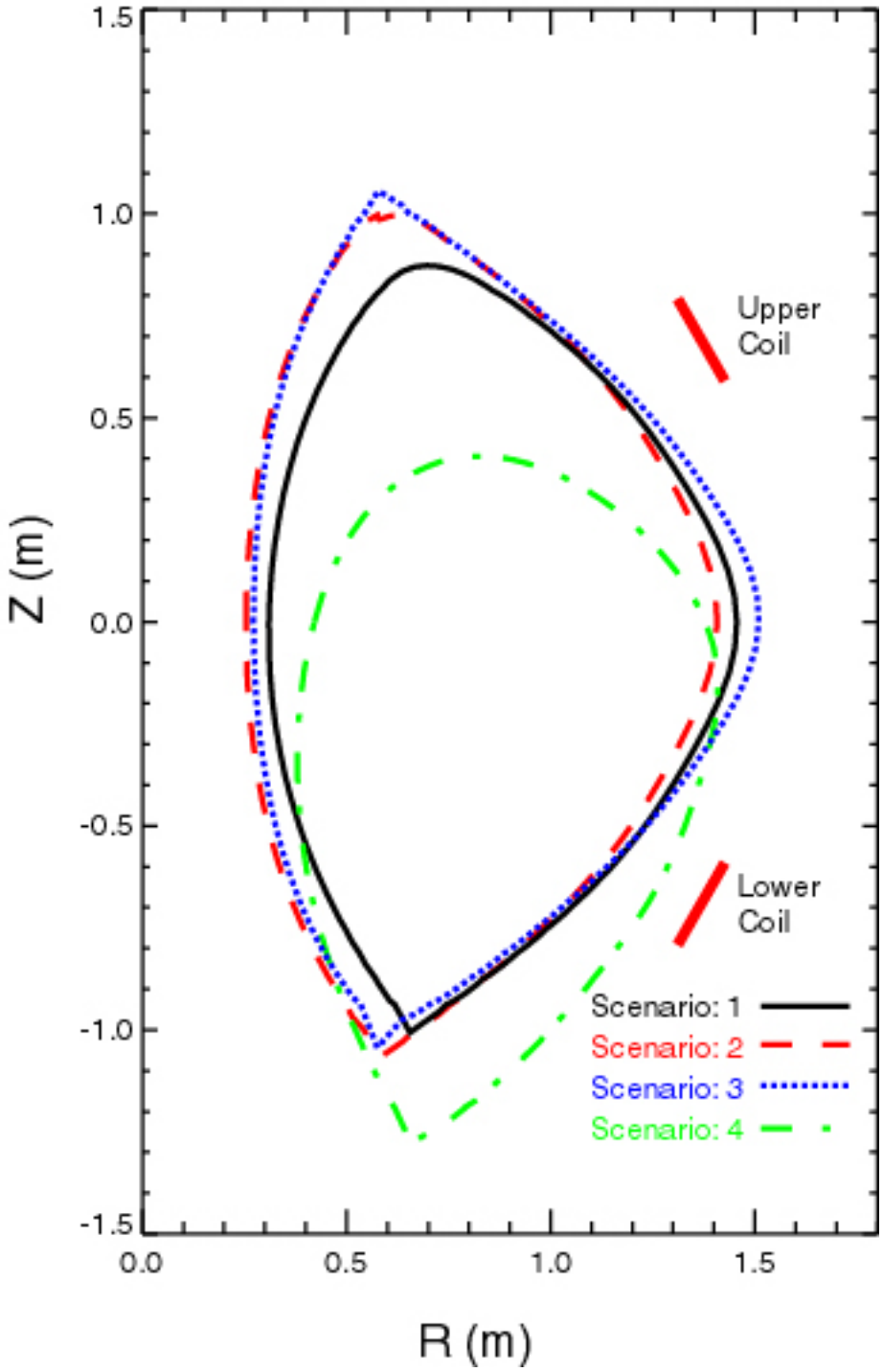

Figure 1 Poloidal profiles of the discharge scenarios. The location of the internal coils is also indicated. The external coils have a height of 4m and are located at a radius of 2.9 m.

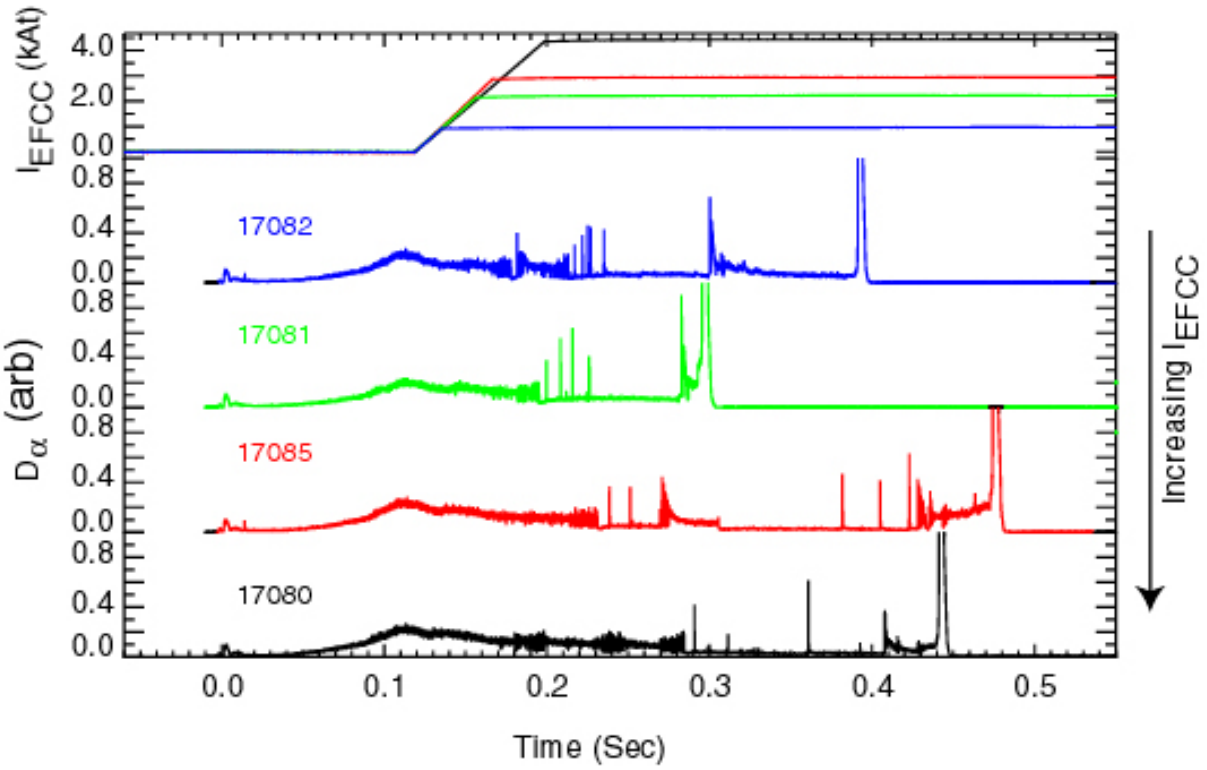

Figure 2 Effect of increasing n=1 error field correction current on the time of the L-H transition for a "scenario 2" discharge.

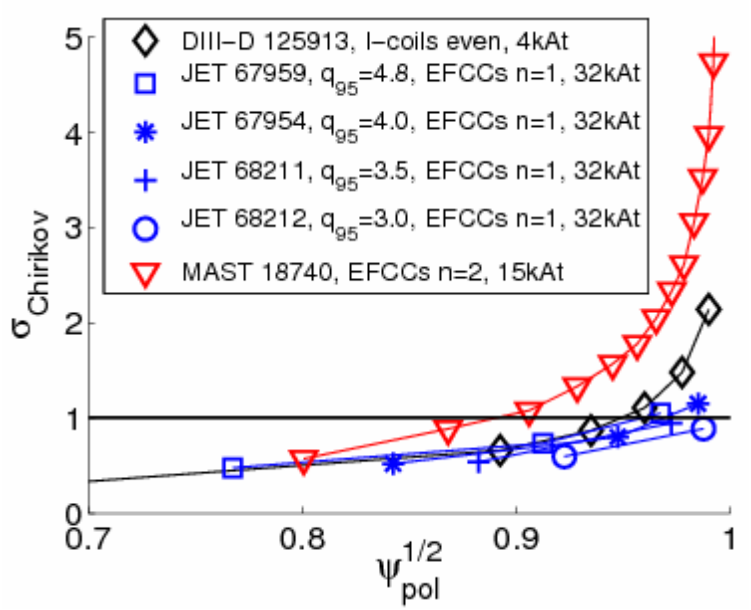

Figure 3 Calculated Chirikov parameter profiles for a MAST "scenario 2" discharge using the external coils in a n=2 configuration. Superimposed are the profiles for DIII-D and JET discharges in which ELM mitigation has been established.

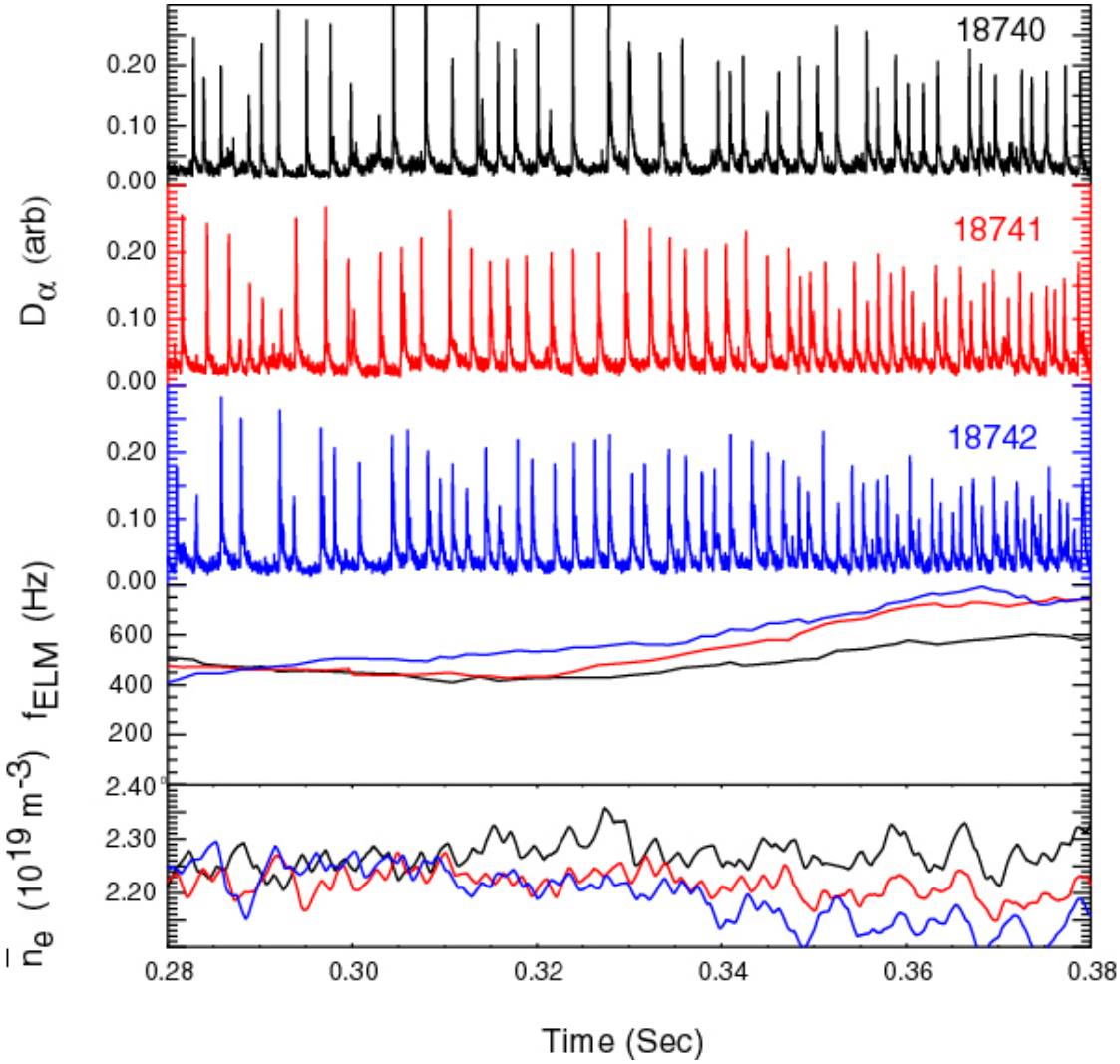

Figure 4 Effect of increasing n=2 error field correction current on a "scenario 3" H-mode plasma: The target D_α, ELM frequency (f_{ELM}) and line averaged density ($\bar{n}_e$) as a function of time.

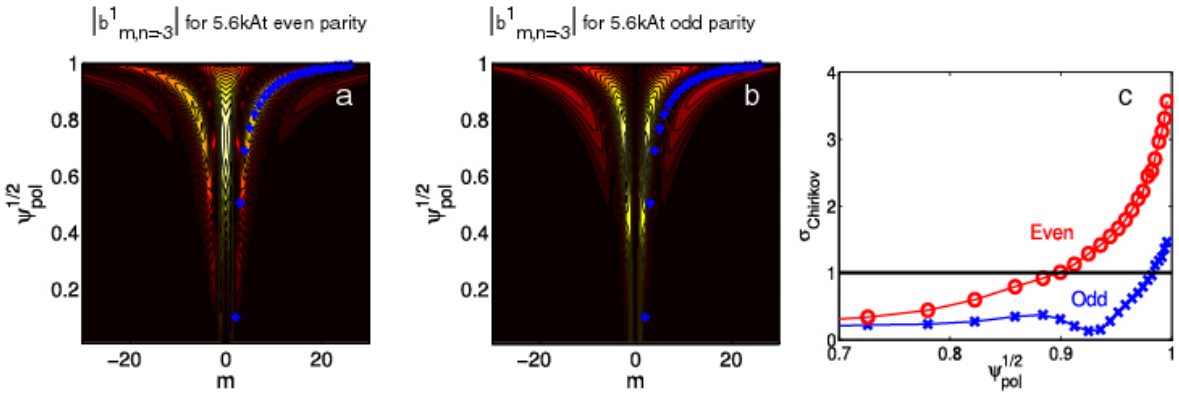

Figure 5 Poloidal magnetic spectra for the a) even and b) odd parity configurations for a "scenario 1" discharge. Superimposed as crosses are the q=m/3 rational surfaces of the discharge equilibrium.c) Predicted profiles of the Chirikov parameter produced with 5.6 kA.t in the internal ELM coils in even (open circles) and odd (crosses) parity configurations.

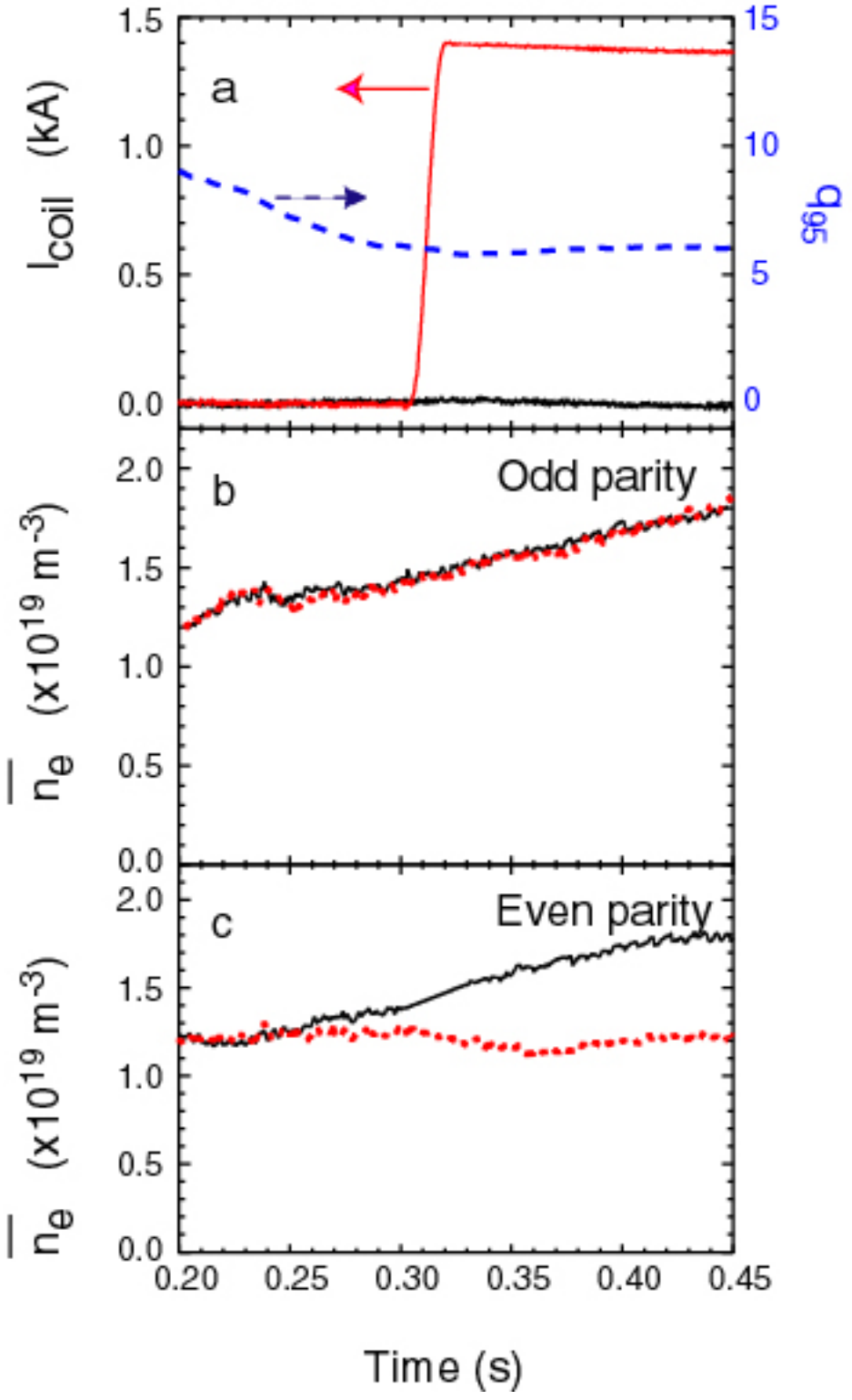

Figure 6 Ohmic shot (scenario 1) with 400 kA plasma current using the internal coils in Odd and Even parity mode. a) the applied coil current (solid - LH axis) and q_{95} (dashed - RH axis). The line average density in b) Odd and c) Even parity mode shots with 0 (solid) and 1.4 kA (dashed) current in the coils.

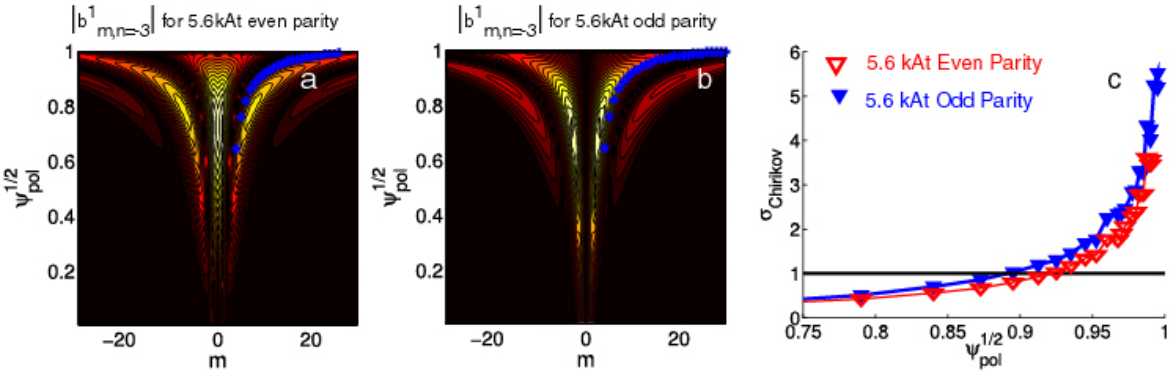

Figure 7 Poloidal magnetic spectra for the a) even and b) odd parity configurations for a "scenario 2" discharge. Superimposed as crosses are the q=m/3 rational surfaces of the discharge equilibrium.c) Predicted profiles of the Chirikov parameter produced with 5.6 kA.t in the internal ELM coils in even (open triangles) and odd (solid triangles) parity configurations.

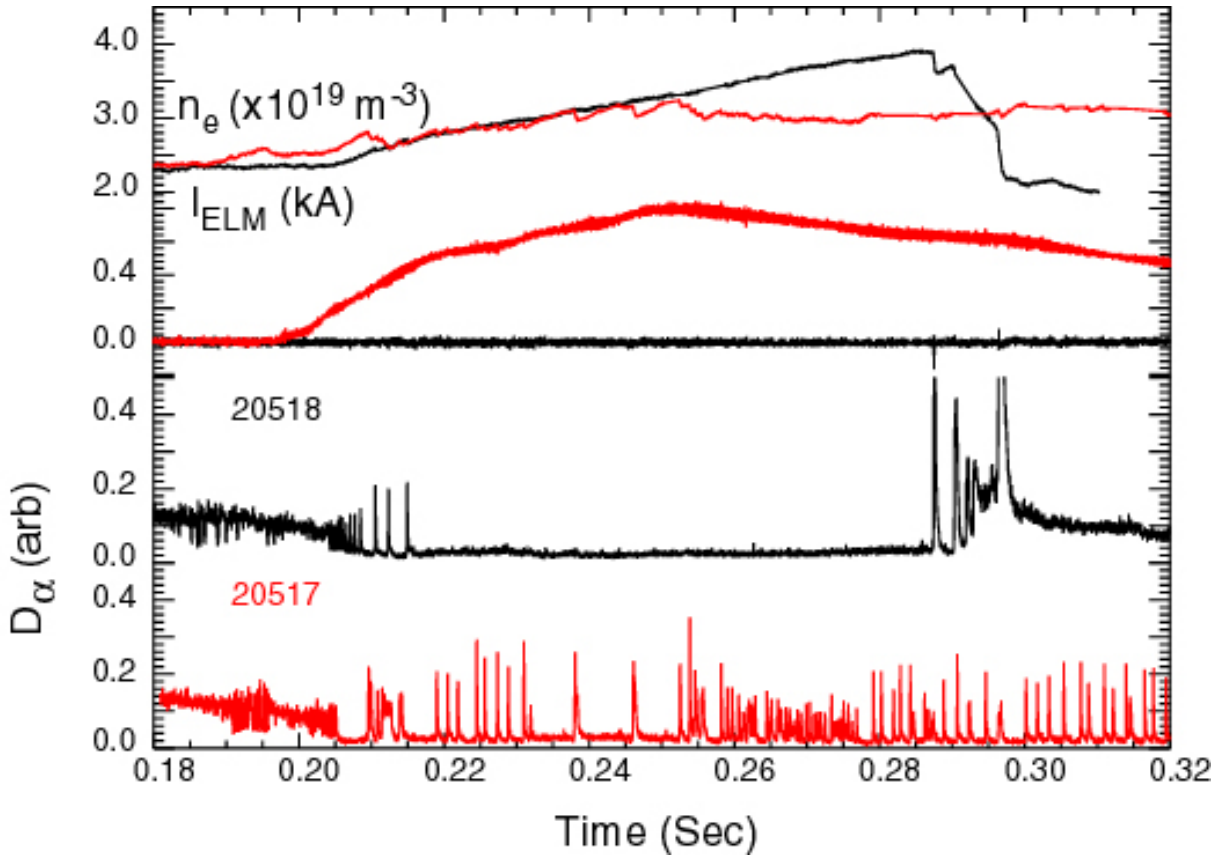

Figure 8 Comparison of "scenario 2" discharges with and without application of the internal coils in odd parity: line averaged density ($\bar{n}_e$), coil current (I_{ELM}) and target D_α as a function of time.

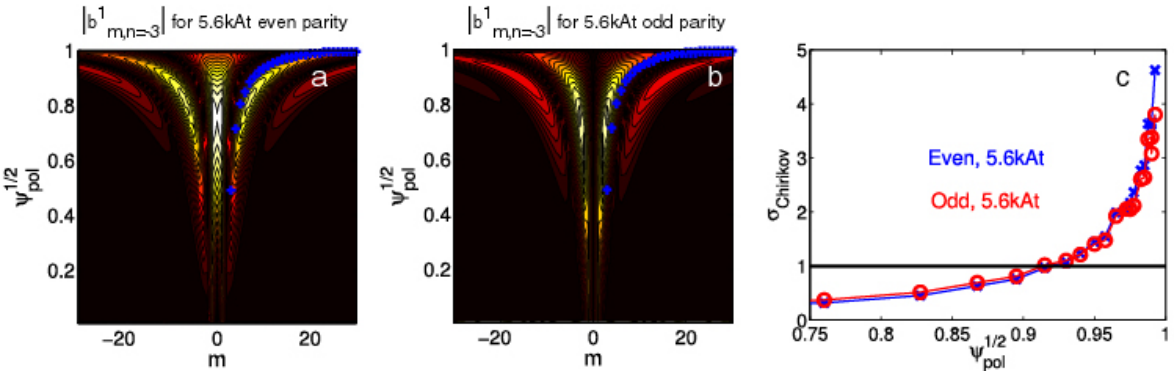

Figure 9 Poloidal magnetic spectra for the a) even and b) odd parity configurations for a "scenario 3" discharge. Superimposed as crosses are the q=m/3 rational surfaces of the discharge equilibrium.c) Predicted profiles of the Chirikov parameter produced with 5.6 kA.t in the internal ELM coils in even (open circles) and odd (crosses) parity configurations.

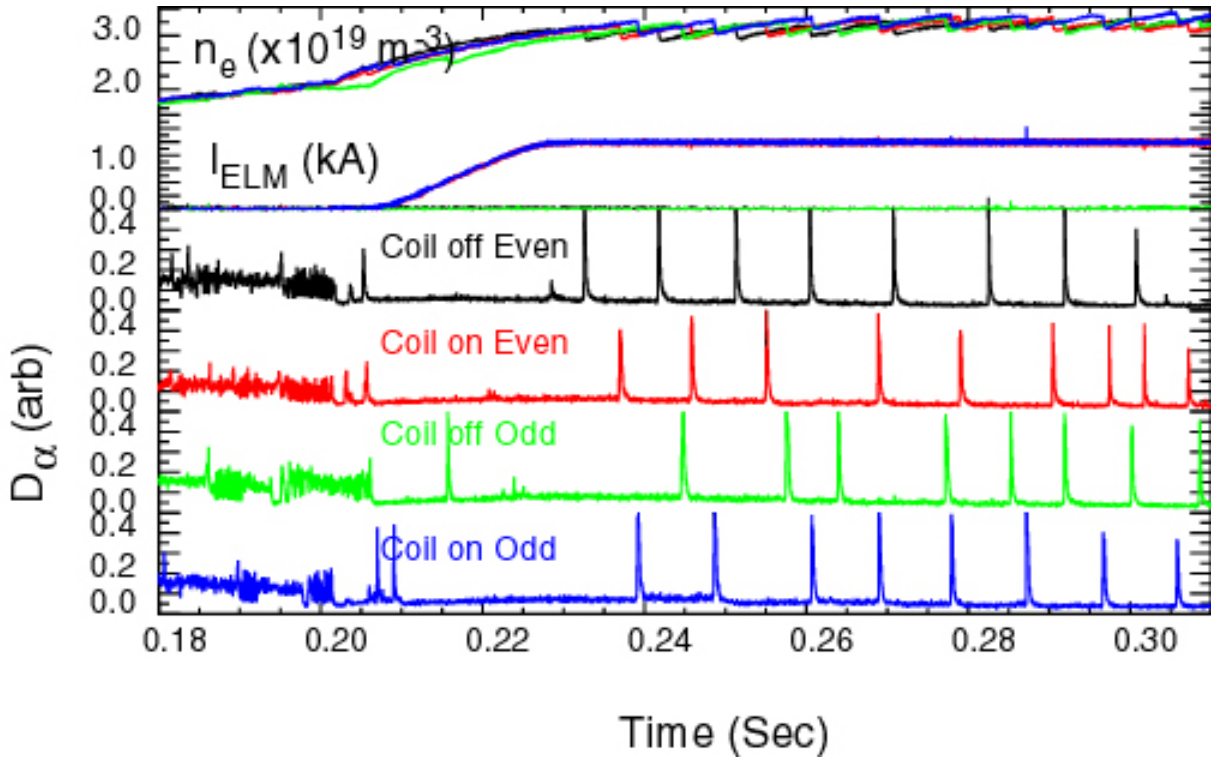

Figure 10 Time traces of line average density ($\bar{n}_e$), coil current (I_{ELM}) and D_α for a 3.2 MW Beam heated H-mode shot (Scenario 3) using the internal coils in even or odd parity mode.

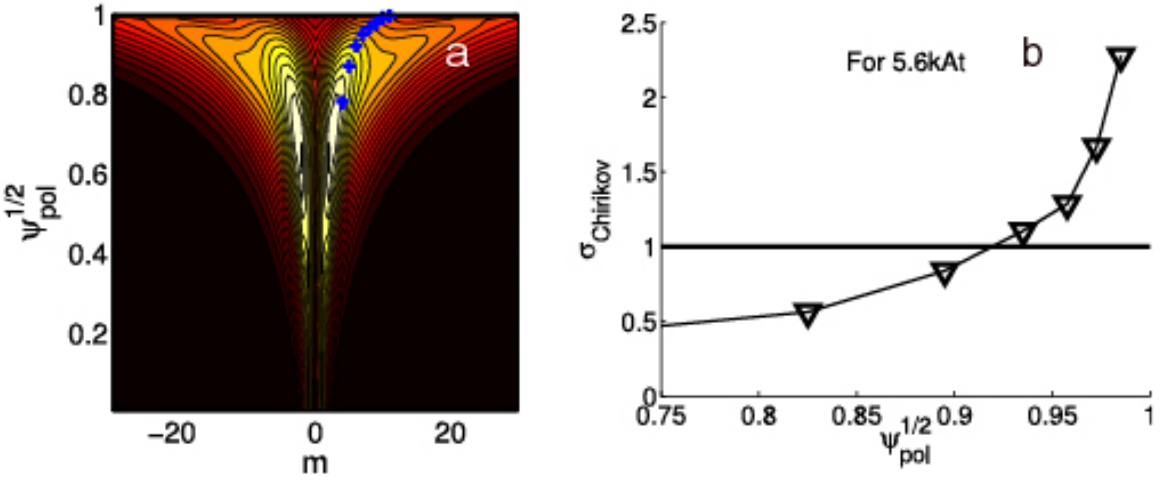

Figure 11 a) Poloidal magnetic spectra for the lower row of coils a "scenario 4" discharge. Superimposed as crosses are the q=m/3 rational surfaces of the discharge equilibrium.
b) Predicted profile of the Chirikov parameter produced with 5.6 kA.t in the internal ELM coils.

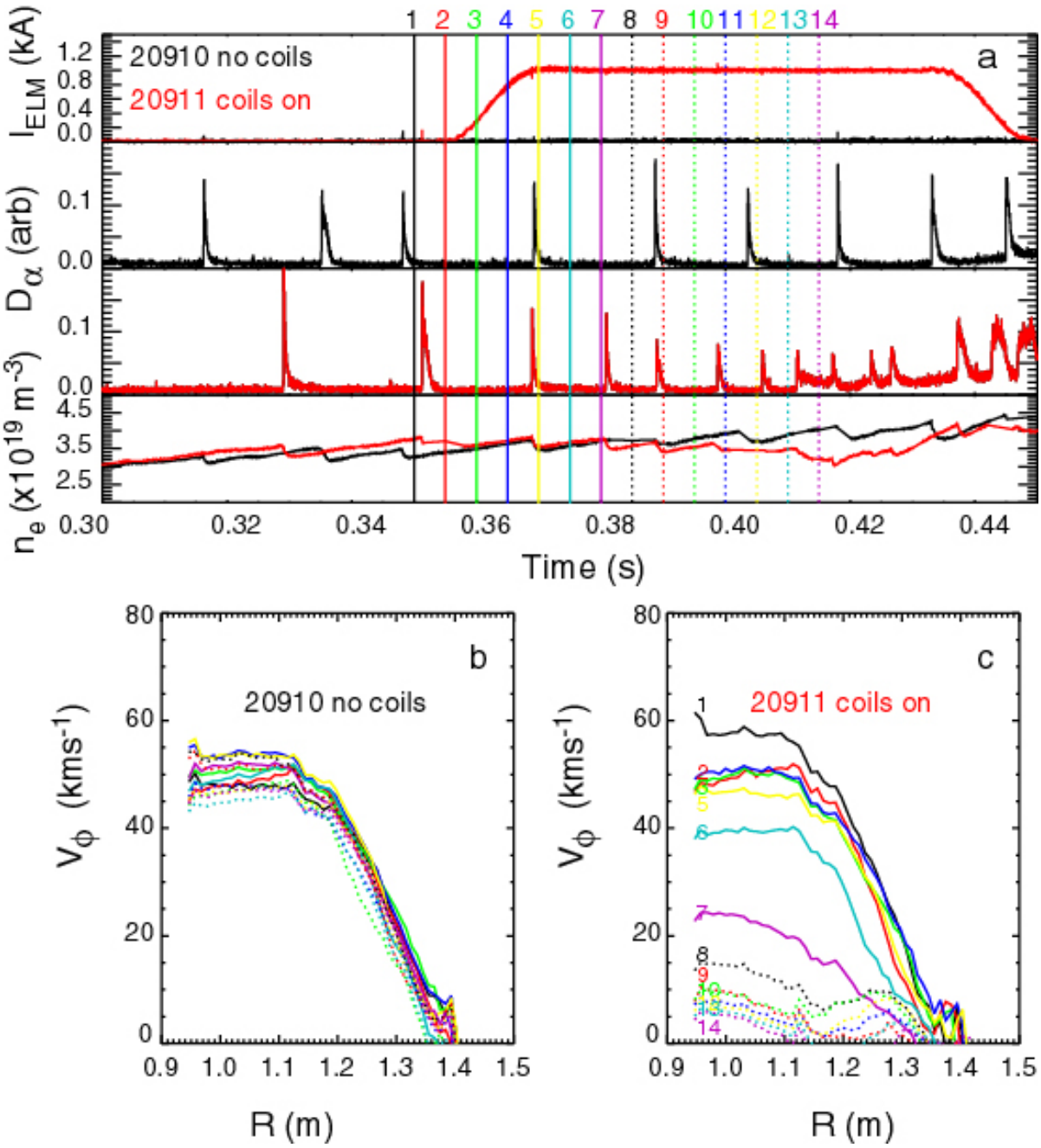

Figure 12 a) Time traces of coil current (I_{ELM}), target D_α and line average density ($\bar{n}_e$) for a 3.2 MW beam heated H-mode shot (Scenario 4) using the lower row of the internal coils. b) and c) radial profiles of the toroidal velocity (V_ϕ) for the time period shown in a) for discharges with and without current in the coils respectively.